International Journal of Pharmaceutics 390 (2010) 225–233

Contents lists available at ScienceDirect

International Journal of Pharmaceutics

journal homepage: www.elsevier.com/locate/ijpharm

Pharmaceutical Nanotechnology

SLN for topical application in skin diseases—Characterization of drug–carrier and carrier–target interactions

Sarah Küchler[a], Werner Herrmann[a], Grazyna Panek-Minkin[b], Tobias Blaschke[b], Christian Zoschke[a], Klaus D. Kramer[b], Robert Bittl[b], Monika Schäfer-Korting[a,*]

[a] Institut für Pharmazie, Freie Universität Berlin, Berlin, Germany
[b] Institut für Experimentalphysik, Freie Universität Berlin, Berlin, Germany

ARTICLE INFO

Article history:
Received 1 December 2009
Received in revised form 1 February 2010
Accepted 4 February 2010
Available online 11 February 2010

Keywords:
Solid lipid nanoparticles
Electron spin resonance
Spin probes
Skin penetration
Drug–carrier interaction
Carrier–target interaction

ABSTRACT

The modes of drug–particle interactions considerably influence drug delivery by nanoparticulate carrier systems and drug penetration into the skin. The exact mechanism of the drug loading and its release are still ambiguous. Therefore, the loading process, the interaction of the agent and the lipid matrix of solid lipid nanoparticles (SLNs) as well as the uptake of the loaded agent by skin lipids were analysed by electron spin resonance (ESR) and parelectric spectroscopy (PS) using spin probes (TEMPO, TEMPOL, and CAT-1) as model drugs differing in their lipophilicity. The spin probes were closely attached to the particles lipid surface (TEMPO) or located in the layers of the surfactant (CAT-1), respectively. Furthermore, two distinct sub-compartments on the SLN were found. To simulate the processes at the phase boundary SLN dispersion/skin, skin lipid mixtures were prepared and the transfer process of the spin labels was followed by ESR tomography. Transfer rates were related to the lipophilicity of the spin probe, the lipid mixture and the applied pharmaceutical formulation, SLN dispersion and aqueous solution, respectively. In particular, SLN accelerated in particular the distribution of the lipophilic agents.

1. Introduction

To improve the notoriously low drug absorption of drugs from the skin surface nanoparticulate carrier systems (e.g. lipid nanoparticles, liposomes, and microemulsions) were proven to be efficient (for review see Schäfer-Korting et al., 2007). Amongst others solid lipid nanoparticles (SLNs) appear to be very promising. SLN dispersions are of superior stability as compared to liposomes (Manjunath et al., 2005; Müller et al., 2002) and uptake enhancement, efficacy and local tolerability of SLN were shown repeatedly (Chen et al., 2006; Kalariya et al., 2005; Küchler et al., 2009b; Kuntsche et al., 2008; Lombardi Borgia et al., 2005; Santos Maia et al., 2002; Stecova et al., 2007). Since skin lipids (epidermal lipids and sebum) build up the penetration barrier a lipid exchange of the particles with the skin surface was hypothesized as drug delivery mechanism and, in fact, intensive interactions of SLN with the skin surface were detected (Küchler et al., 2009b; Kuntsche et al., 2008). Yet, the processes at the phase interface SLN/skin surface are not completely known, the nature of the carrier matrix and the mode of drug interaction with the lipid matrix proved relevant. For example, drug attachment to the SLN surface can allow for a targeting to epidermal structures (Santos Maia et al., 2002; Sivaramakrishnan et al., 2004; Stecova et al., 2007). This may be linked to the drug release patterns of SLN. Burst release and prolonged release, respectively, are explained by different drug distribution profiles within the lipid carriers. Drug-enrichment in the superficial layers of SLN or on its surface can result in burst release, whereas prolonged release indicates intensive drug–lipid interactions and drug localization in the core of the SLN (Müller et al., 2000; zur Mühlen et al., 1998). Yet, also tensids used for particle stabilization can affect the drug release considerably as observed with amiodaron loaded lipid nanocapsules (Lamprecht et al., 2002).

Actually, predicting and regulating the drug distribution in the lipid matrix and, hence, the drug release profile is quite difficult. A detailed insight becomes possible by electron spin resonance (ESR) imaging. For this purpose, spin probes are loaded to SLN and the measured individual rotational correlation times τ_R reflect the mobility of the spin probes. Low τ_R indicates high mobility and thus, most likely, an attachment of the spin probe to the particle surface. In contrast, very high τ_R indicates for a spin probe incorporation in the lipid matrix. Furthermore, using the highly lipophilic cholestane probe recent studies revealed two sub-compartments of

Abbreviations: A_{iso}, hyperfine splitting constant; c, concentration of the model drugs; $\Delta\varepsilon(c)$, dipole density; $f_o(c)$, dipole mobility; ESR, electron spin resonance; LD, laser diffraction; PCS, photon correlation spectroscopy; PI, polydispersity index; PS, parelectric spectroscopy; τ_R, rotational correlation time; SCS, stratum corneum substitute; SLN, solid lipid nanoparticle(s).

* Corresponding author at: Institut für Pharmazie, Königin-Luise-Str. 2-4, D-14195 Berlin, Germany. Tel.: +49 030 838 53284; fax: +49 030 838 54399.
E-mail address: msk@zedat.fu-berlin.de (M. Schäfer-Korting).

0378-5173/$ – see front matter © 2010 Elsevier B.V. All rights reserved.
doi:10.1016/j.ijpharm.2010.02.004

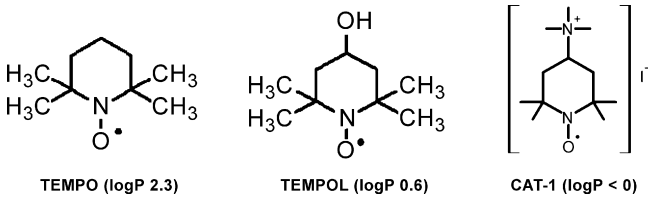

Fig. 1. Structure and lipophilicity (log *P*) of the spin probes.

SLN: attachment to the flat surface (low cholestane probe mobility) and to the rim of disc-like SLN (higher mobility), respectively (Braem et al., 2007). Yet, the preconditions for drug incorporation or attachment are still ambiguous. Besides the drug–carrier interaction, ESR imaging is also a valuable tool to study physicochemical properties of biological systems, drug distribution in multiphase systems and processes taking place at phase boundaries including skin penetration (Herrmann et al., 2007; Moll et al., 2008).

The first aim of this study was to unravel the loading of SLN and the drug localization in relation to the lipophilicity of the loaded agents. Thus, the spin probes TEMPO, TEMPOL and CAT-1 (Fig. 1) were chosen due to their comparable basic structures with similar molecular volumes but widely varying lipophilicity. Furthermore, we aimed to simulate the processes at the phase interface pharmaceutical formulation/skin in relation to the physicochemical properties of the drug and the acceptor. Hence, the transfer of the spin probes from the formulation into two lipid matrices mimicking the lipids of the skin surface (artificial skin sebum mixture and stratum corneum substitute) was studied by ESR tomography.

2. Materials and methods

2.1. Materials

Compritol® 888 ATO (glyceryl behenate) was a gift from Gattefossé (Weil a. Rh., Germany), the tensid Lutrol F68® (Poloxamer 188®) was obtained from BASF (Ludwigshafen, Germany). The nitroxide spin probes 2,2,6,6-tetramethylpiperidin-1-oxyl (TEMPO, log *P* 2.3) and 2,2,6,6-tetramethyl-4-trimethylammoniumpiperidin-1-oxyl-iodide (CAT-1, log $P \leq 0$) were purchased from the Institute of Organic Chemistry, Russian Academy of Science (Novosibirsk, Russia). 4-Hydroxy-2,2,6,6-tetramethylpiperidin-1-oxyl (TEMPOL, log *P* 0.6), the components of the artificial sebum and the components of the stratum corneum substitute (SCS) were obtained from Sigma–Aldrich (Munich, Germany), except where noted. Pork lard came from Caelo (Hilden, Germany), Witepsol® H5 from Sasol (Witten, Germany) and the ceramides I, III and VI from Evonik (Essen, Germany).

2.2. Particle preparation

SLNs, composed of 10% solid lipid (Compritol® 888 ATO) and 2.5% surfactant, were prepared as described (Lombardi Borgia et al., 2005). In short, the spin probes TEMPO and TEMPOL were dissolved in the melted lipid at 95 ± 5 °C. An aqueous solution of Poloxamer 188® of the same temperature was added and a pre-emulsion was formed using a rotor–stator mixer. The hydrophilic CAT-1 was dissolved in the aqueous tensid solution and then added to the melted lipid. The premix was homogenized by an Emulsiflex C5 high pressure homogenizer (Avestin, Mannheim, Germany) at 500 bar for 2.5 min. Concentrations of the spin probes of the SLN dispersions as well as the aqueous solution used for reference were as follows: TEMPO 0.0055–0.1%, TEMPOL and CAT-1 0.0055–0.025%. SLNs were stored at 8 °C protected from light and used for tests within 1 month.

2.3. Particle characterization

Photon correlation spectroscopy (PCS; Malvern Zetasizer ZS, Malvern Instruments, Malvern, UK) was used for SLN size characterization (*z*-average) and the polydispersity index, PI. Larger particles with micrometer size were detected by laser diffraction (LD; Coulter LS 230, Miami, FL, Müller et al., 2002). Differential scanning calorimetry (DSC) was performed on a Mettler DSC 821^e (Mettler Toledo, Gießen, Germany). The SLN dispersions were weighted in 40 μl aluminum pans. DSC scans were recorded at a cooling rate of 5 °C/min down to 193 K.

2.4. Interaction of spin probes and the particles: parelectric spectroscopy and ESR spectroscopy

Parelectric spectroscopy (PS) was applied in order to exclude free spin probes in the aqueous phase of SLN dispersions. The theoretical background is described in detail elsewhere (Blaschke et al., 2007; Braem et al., 2007).

ESR spectroscopy was performed to obtain a more detailed insight into the loading process of SLN in relation to the physicochemical properties of the loaded agents. Therefore, ESR spectra of SLN loaded with various concentrations of the spin probes were recorded on a laboratory-built X-band spectrometer (microwave bridge ER 041 MR, BRUKER, Germany, electromagnet AEG, Berlin, Germany, lock-in amplifier Stanford Research 810, Stanford, USA). The SLN dispersions were studied at temperatures from 273 K down to 213 K under non-saturating conditions. Spectra were submitted to a complete line-shape analysis according to Freed's interpretation (Budil et al., 1996). Additionally, the hyperfine splitting constant A_{iso} for TEMPO, TEMPOL and CAT-1 in water, SLN and Compritol® were measured to obtain information about the microviscosity of the environment of the spin probes and, thus, to distinguish between a drug incorporation in the lipid matrix or an attachment to the particle surface.

2.5. ESR tomography

In order to examine the distribution processes at phase interfaces spectral–spatial ESR imaging was carried out. The spectra were recorded using an X-band spectrometer (ERS 220, ZWG, Berlin, Germany) with a homebuilt imaging extension (Herrmann et al., 2007). The samples were measured in a common TE_{102} cavity with the following settings: microwave frequency, 9.5 GHz; microwave power, 5 mW; modulation amplitude, 0.2 mT; scan width, 8 mT; maximum gradient, 4.68 T/m; scan time per projection, 10 s; number of projections, 95; missing 12; points per projection, 512. Filtered backprojection was used for image reconstruction giving an image matrix of 256 × 256 points. The cavity temperature was set to 32 °C, the surface temperature of the normal skin (Schäfer-Korting et al., 2007). Aqueous solutions and SLN dispersions with TEMPO (0.1%), TEMPOL (0.025%) and CAT-1 (0.025%) were tested, respectively.

In order to unravel the factors influencing the processes at the phase interface formulation/skin an artificial sebum and a stratum corneum substitute (SCS) were prepared. For the artificial sebum pork lard (34%), stearic acid (25%), lanolin (23%), squalene (12%), cholesterol (4%) and cholesterol sulfate (2%) were melted in a water bath and stirred until homogeneity (Musial and Kubis, 2003). The stratum corneum substitute was composed of a fatty acids mixture (25%), cholesterol (20%), cholesterol oleate (10%), Witepsol® H5 (=triglycerides, 20%) and a ceramide mixture (25%). The ceramides I (5.6%), III (27%) and VI (67.4%) were used. For the fatty acid mixture, myristic acid (2.4%), palmitic acid (38.3%), stearic acid (10.7%), palmitoleic acid (2.7%), oleic acid (33.5%) and linoleic acid (12.4%) were blended by carefully melting on a water bath at 75 °C (Jaeckle

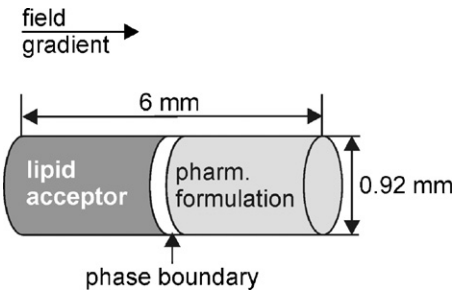

Fig. 2. Experimental arrangement of the ESR tomography measurements.

et al., 2003). The lipid mixtures were stored at 2–8 °C, respectively, and used for 1 month.

The investigation of the phase interface processes was performed according to the arrangement displayed in Fig. 2. The acceptor lipid was transferred in the molten state into the capillary and was carefully overlaid with the formulation avoiding air bubbles at the interface region.

3. Results

3.1. Particle characterization

Particle size and size distribution of the spin probe-loaded SLN were measured by PCS and LD. PCS measurements showed an average size of 170–190 nm for the SLN loaded with TEMPO and TEMPOL. Interestingly, clearly larger particles of 250–420 nm in size were obtained when loading CAT-1. Increasing CAT-1 concentrations resulted in larger particles. Furthermore, the stability of the CAT-1 SLN was influenced by the spin label concentration. Concentrations ≥0.05% facilitated an immediate gelation of the SLN dispersion and those suspensions were excluded from further investigations. The particle sizes of TEMPO-/TEMPOL-SLN showed no concentration dependency; the PI was <0.250, respectively. Micron-sized particles were not detected by LD measurements.

DSC was performed in order to detect changes in the lipid structure of SLN during cooling down below the freezing point as also done for the ESR measurements. The recorded DSC runs displayed an exothermic peak at temperatures about 250–260 ± 5 K, respectively. This peak most likely depicts the freezing point of the dispersion, as in consequence of high amounts of dispersed or dissolved substances the freezing point is significantly lowered.

Table 1
The rotational correlation time τ_R at 213 K in dependence on the spin probe (0.0065%).

	τ_R (high mobility)	τ_R (low mobility)
TEMPO	23 ns	74 ns
TEMPOL	26 ns	178 ns
CAT-1	109 ns	252 ns

Table 2
The hyperfine splitting constant A_{iso} of the spin probes in water, Compritol® and SLN.

	TEMPO	TEMPOL	CAT-1
Water	1.664	1.641	1.621
Compritol®	1.492	1.469	–
SLN	1.66	1.637	1.625

3.2. Interaction of spin probes and the particles: parelectric spectroscopy and ESR spectroscopy

3.2.1. Parelectric spectroscopy

PS measurements in the frequency region 0.4–4.0 GHz were performed in order to exclude free molecules of the hydrophilic CAT-1 in the water phase of the SLN and to ensure high loading capacity. No CAT-1 molecules were detectable suggesting complete drug loading of the SLN.

3.2.2. ESR spectroscopy

Former studies revealed two sub-compartments of the disc-like SLN (Braem et al., 2007). This also holds true for the SLN loaded with TEMPO, TEMPOL and CAT-1, respectively, as depicted exemplarily for TEMPO-SLN in Fig. 3. At low temperatures (213–245 K), measurements of SLN loaded with TEMPO showed two correlation times, a lower with τ_R = 10–25 ns, meaning a higher mobility and a higher with τ_R = 70–140 ns, meaning lower mobility, with roughly equal relative contributions (Fig. 4). The percentages of the correlation times significantly changed at a temperature around 255 K (Fig. 4) coinciding with the peak in the DSC measurements. These results hold true for TEMPOL and CAT-1 loaded SLN, too. In contrast to TEMPO, however, higher values of τ_R were measured with TEMPOL and, even more pronounced, CAT-1 (Table 1). Mobility is least with CAT-1.

To distinguish between drug incorporation in the lipid matrix of SLN and an attachment to the particle surfaces A_{iso} values were determined. In water and SLN A_{iso} was about 1.64 ± 0.015 for TEMPO, TEMPOL and CAT-1, respectively (Table 2). In Compritol®

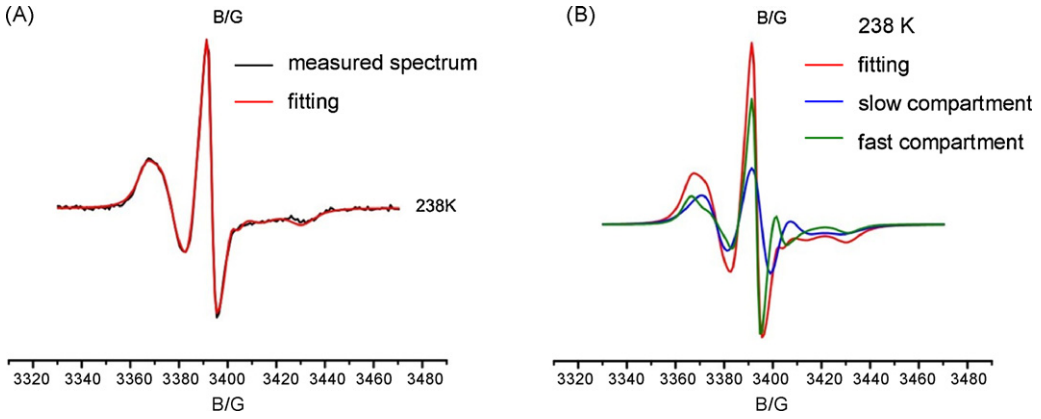

Fig. 3. The conformity of measured and fitted (sum of the slow and fast spectra) ESR spectrum is depicted in A (exemplary at 238 K). Two distinct sub-compartments of spin label sites conducting different rotational mobility of the molecules (TEMPO-SLN 0.01%) computed by line-shape analysis according to Freed (Budil et al., 1996) (B). The results were confirmed with at least three independent experiments, respectively.

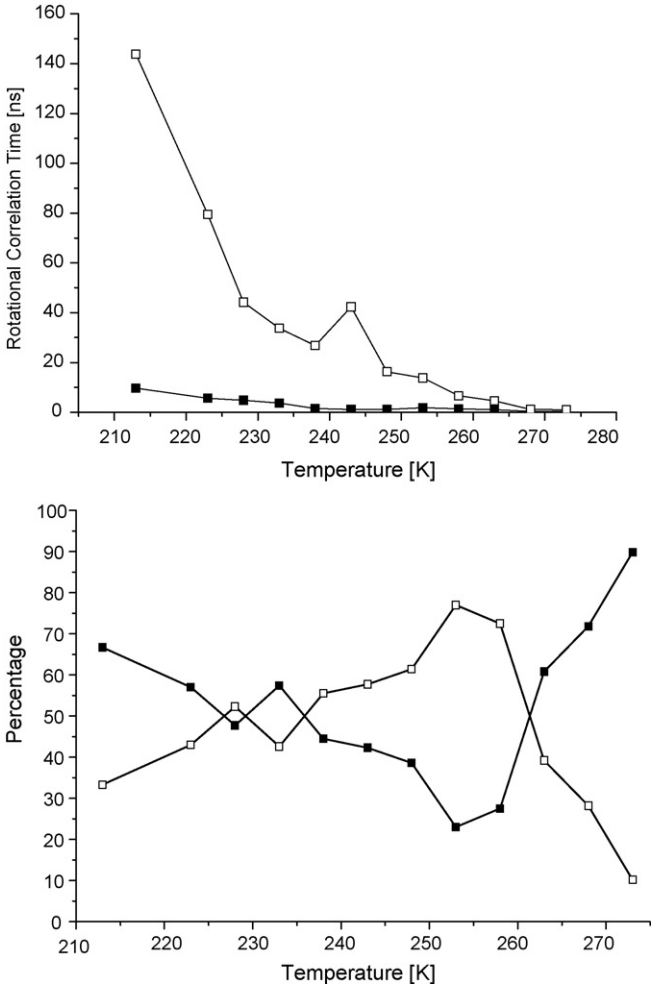

Fig. 4. Different rotational correlation times τ_R and thus mobility of TEMPO molecules loaded onto SLN (0.01%) indicates two sub-compartments of localization on SLN (■ = fast compartment, □ = slow compartment). By increasing the temperature, the percentages of the molecules in the sub-compartments change. The results were confirmed by measurements of independent SLN batches and, additionally, varying spin probe concentrations (0.005–0.01%).

values about 1.48 ± 0.011 were measured for TEMPO and TEMPOL, no values could be specified for CAT-1.

3.3. ESR tomography

Next we studied the relation of spin probes loaded onto SLN and its transfer to skin substitutes (Figs. 5–7). The processes at the phase boundaries were surveyed up to 24 h to obtain information about the time dependence of the test compound distribution into the lipid acceptor phase. The shown ESR spectra depict no equilibrium state but the time point of first relevant changes.

The diffusion of TEMPO from the formulations into artificial sebum and the SCS proceeded almost completely and very quickly. Already after 5 min a remarkable amount had penetrated into the lipid, after 2 h, at the latest, the distribution process was almost finished (Fig. 5). As to be anticipated from skin penetration of lipophilic agents (Kalariya et al., 2005; Küchler et al., 2009b; Lombardi Borgia et al., 2005; Stecova et al., 2007) SLN accelerated the diffusion of TEMPO significantly compared to the aqueous solution (Fig. 5). With TEMPOL the transfer into the artificial sebum proceeded slowly, after 3.5 h small amounts were detectable in the lipid mixture but only after application of the SLN (Fig. 6). In contrast, no TEMPOL distribution was observed in the SCS. Considering CAT-1, following the application of the aqueous solution, a slight amount was detectable in the sebum after 8.5 h (Fig. 7). Interestingly, less spin probes were penetrated within the same time after application of the CAT-1 loaded SLN. No diffusion into the SCS could be detected with the CAT-1 solution and SLN.

4. Discussion

Solid lipid nanoparticles improve the skin penetration and tolerability of various topically applied drugs (Chen et al., 2006; Kalariya et al., 2005; Santos Maia et al., 2002; Schäfer-Korting et al., 2007; Stecova et al., 2007). Interestingly, SLN can induce epidermal targeting (Chen et al., 2006; Santos Maia et al., 2002; Stecova et al., 2007), too. Therefore it is important to understand the loading process, particle structure and particle–drug interactions to enable a prediction of the drug release, penetration and effectiveness at the skin. The close relation of intracutaneous distribution and the location of the agents in the formulation – whether incorporated into the lipid matrix or attached to the particle surface – was already shown (Lombardi Borgia et al., 2005; Santos Maia et al., 2002; Stecova et al., 2007). By applying the methods of ESR and TEM more detailed insight was obtained about the structure of SLN and the localization of the highly lipophilic spin probes in those carriers (Ahlin et al., 2000; Braem et al., 2007; Jores et al., 2003).

Aiming to unravel the loading process and the localization of the loaded agent in dependence on the physicochemical properties the spin labels TEMPO, TEMPOL and CAT-1 of rather similar molecular structure but varying in lipophilicity (Fig. 1) were studied.

Despite of the lower lipophilicity of our test agents, the existence of two sub-compartments on SLN was confirmed, as already described for very lipophilic spin probes (Ahlin et al., 2000; Braem et al., 2007). The ESR spectra (Figs. 3B and 4) displayed one compartment characterized by high rotational mobility and one compartment of lower rotational mobility indicating different locations of the spin probes on the SLN (Table 1). The percentages of the sub-compartments were dependent on the temperature (Fig. 4). At temperatures of about 255 K we observed significant changes in the percentages of the two correlation times indicating a change of the distribution of the spin probes within the SLN, respectively (Fig. 4B). The temperature of this transition is well in accordance with the results of the DSC measurements. The exothermic peak at $250–260 \pm 5$ K marks a change in the structure of SLN, most likely the freezing point. The freezing causes an alteration of the whole system and, thus, a reallocation of the spin label molecules is initiated resulting in the change of the percentages. Thus, we favour the model of a dynamic localization of the spin labels in SLN formulations instead of the idea of fixed drug localization. Thereby, environmental conditions, e.g. the temperature, have great influence and will influence drug release when the formulation is applied onto the skin (Schäfer-Korting et al., 2007). In fact, SLN application to the skin can induce burst release of the loaded drug (Jenning et al., 2000a,b) as well as a major change in the particle structure as to be detected by scanning electron microscopy of pig skin after 0.5–4 h (Küchler et al., 2009b).

In contrast to previous studies (Braem et al., 2007), with less lipophilic agents, however, a clear distinction between the localization on the rim or on the surface of the SLN is not possible here. Though, the A_{iso} values clearly indicate that TEMPO, TEMPOL and CAT-1 are not incorporated into the lipid matrix of the SLN but attached to the particle surface. Values about 1.64 ± 0.015 were obtained in water and in SLN for the three spin probes, respectively, meaning a low viscosity of the microenvironment of the spin probes (Table 2). In contrast A_{iso} values measured in Compritol® were about 1.48 ± 0.011 for TEMPO and TEMPOL indicating high

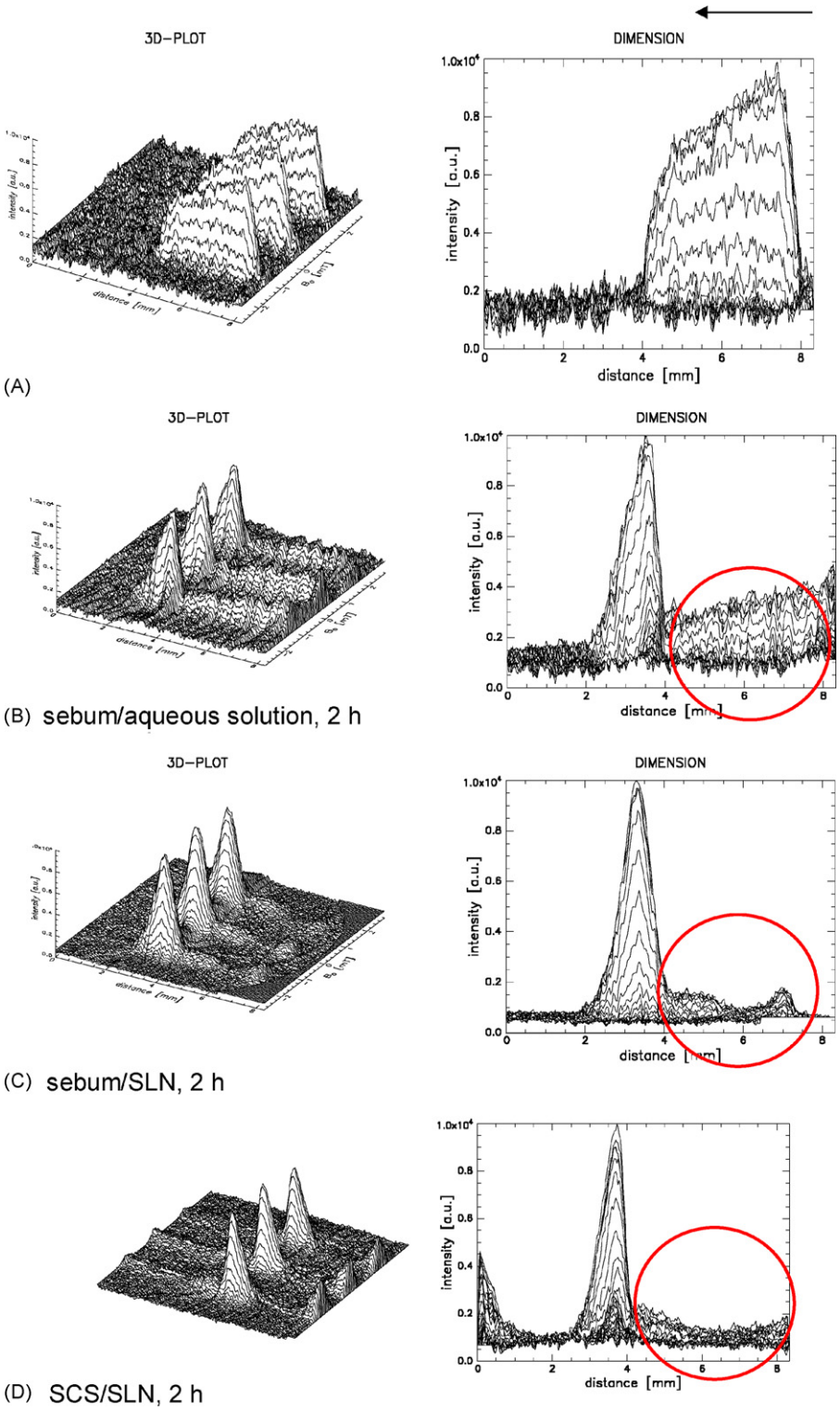

Fig. 5. After 2 h TEMPO was almost completely diffused into sebum and SCS following the application of SLN (C and D). In contrast the diffusion process takes places much slower following the application of the aqueous solution (B). A depicts the starting point; the arrow indicates the direction of spin probe distribution. The amounts of TEMPO not (yet) diffused into the acceptor lipid are encircled. The experiments were repeated twice.

microviscosity. With CAT-1 no evaluable spectra were obtained, most likely due to its hydrophilicity.

Previous studies already demonstrated that lipophilic substances are closely attached to the particle surface (Ahlin et al., 2000; Jores et al., 2003), which is well in accordance with the results for TEMPO in this study. For additional information the evaluation of the rotational correlation time τ_R was proven to be a suitable tool. Comparing the rotational mobility of the sub-compartments of SLN, significantly higher rotational correlation time values were measured for TEMPOL and, even more pronounced, CAT-1 as compared to TEMPO (Table 1). This effect appoints to different locations of the spin probes. The molecules of TEMPO, located at the particle surface have more rotational freedom and are not subject to intense interactions with the aqueous phase. In contrast, we

have to assume that TEMPOL is located in the deeper layers of the Poloxamer covering the SLN surface, whereas CAT-1 is most likely located in the outermost surfactant layers due to its hydrophilicity. These locations condition the rotational mobility of TEMPOL, and in particular, of CAT-1 which is reduced by additional interactions with the Poloxamer and the aqueous phase, as e.g. the formation of hydrogen bonds and in case of CAT-1 even of ionic interactions. Concerning CAT-1 this assumption is affirmed by the increasing particle sizes with higher spin probe concentrations. The ease of gelation in the case of SLN loaded with high

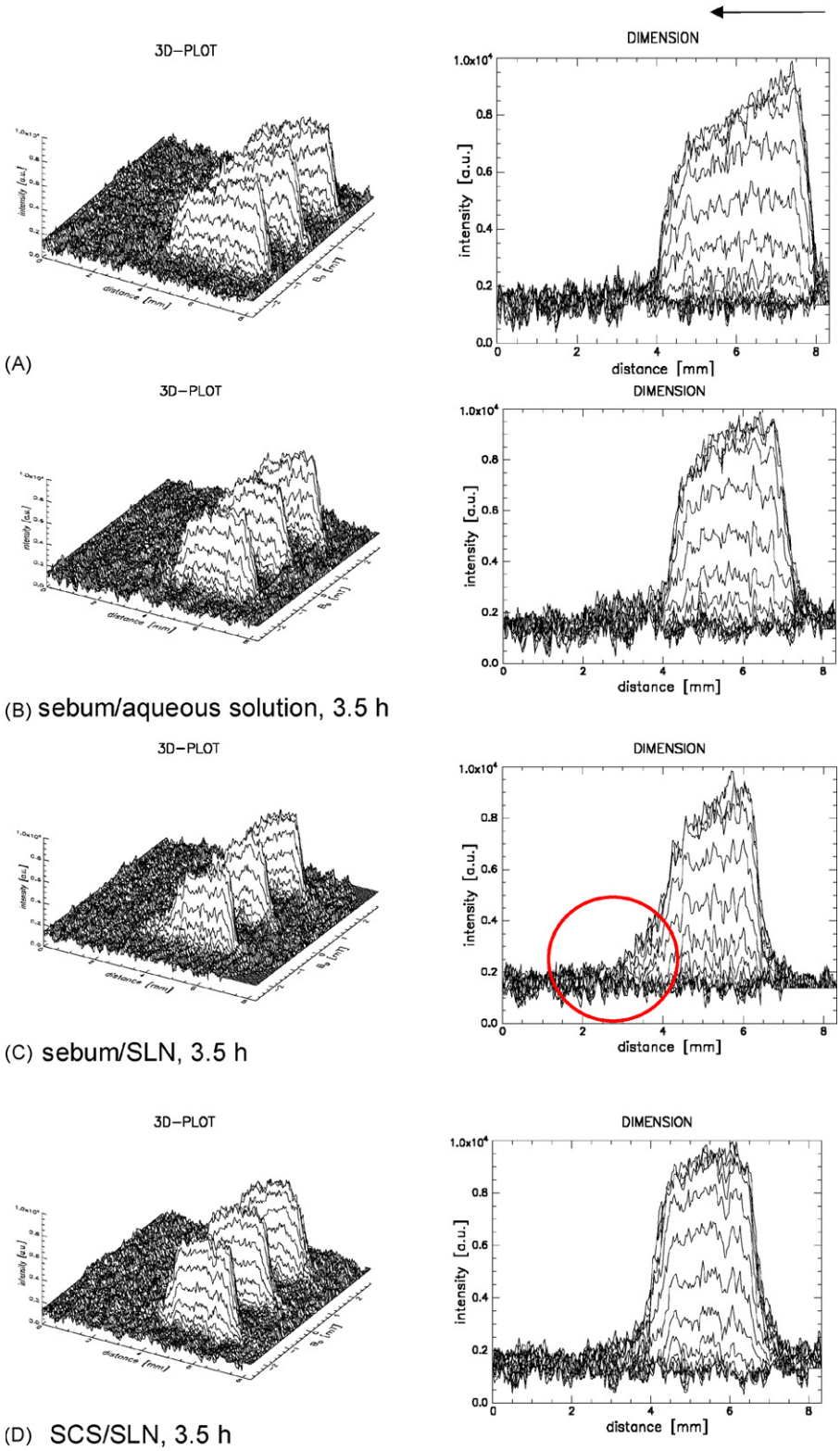

Fig. 6. Primarily after 3.5 h a small amount of TEMPOL was detected in sebum following an application of SLN (C, encircled). No diffusion was observed with the aqueous solution and with SCS as acceptor lipid (B and D). A depicts the starting point; the arrow indicates the direction of spin probe distribution. The experiments were repeated twice.

amounts of CAT-1, is well in accordance with a location close to the aqueous phase. Then, strong interactions with the solvent molecules like hydrogen bonds are possible and, hence, the agglomeration of SLN is facilitated. We observed a concentration-related particle size with another hydrophilic agent, Rhodamin B (Küchler et al., 2009a), too. Moreover, gelation phenomena and the increase in particle sizes when loading higher spin probe amounts onto SLN did not occur with TEMPO or TEMPOL. Our results clearly account for the potential of SLN to serve as drug carriers for hydrophilic drugs, too, although this approach failed with other agents such as a nonsteroidal antiandrogen (Münster et al., 2005).

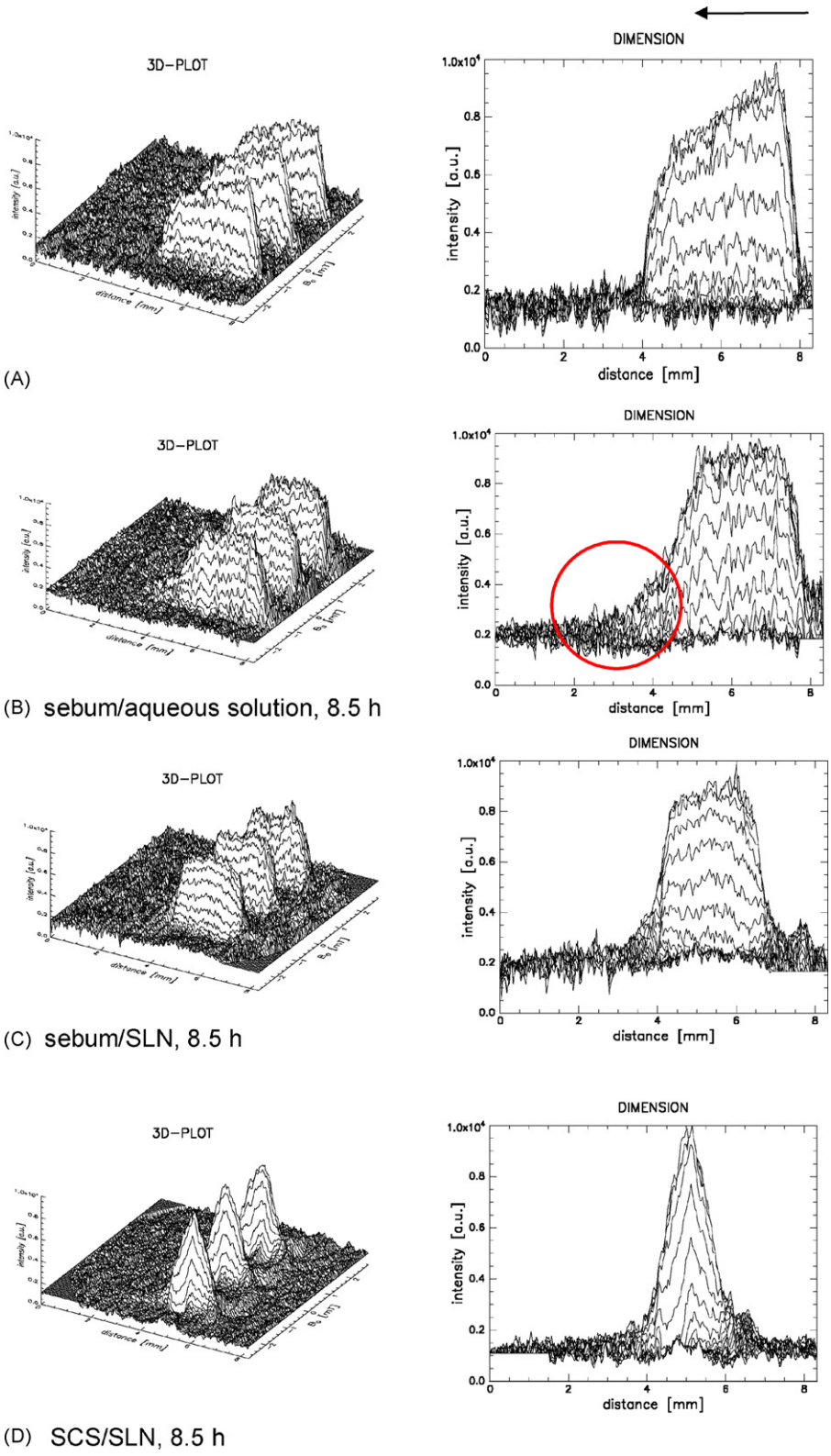

Fig. 7. After 8.5 h CAT-1 had diffused into the sebum out of the aqueous solution (B, encircled). None was diffused following the application of SLN (C and D). A depicts the starting point; the arrow indicates the direction of spin probe distribution. The experiments were repeated twice.

To obtain a clearly more detailed insight into the interactions between SLN formulation and skin, model lipid mixtures were prepared and the processes at the phase boundary after application of a pharmaceutical formulation were studied by ESR tomography. The lipid mixtures proved to mimic *in vitro* the barrier properties of human skin suitably (Jaeckle et al., 2003; Musial and Kubis, 2003). The transfer processes depended considerably on the applied spin probes, the formulation and the lipid acceptor. The spin probes of both SLN and aqueous solution diffused more easily into the sebum as compared to the SCS (Figs. 6 and 7), which we used to mimic the human stratum corneum (Jaeckle et al., 2003). The lipophilic TEMPO penetrated fast and almost completely into all tested lipid mixtures within 2 h (Fig. 5) as TEMPO ($\log P = 2.3$) fits best with the demands of good skin penetration ($\log P = 1–3$) (Degim et al., 2003; Potts and Guy, 1992), whereas the other spin probes are more hydrophilic. Of the rather hydrophilic model agent TEMPOL just a slight amount had diffused into the sebum after 3.5 h and almost no diffusion was observed with the highly hydrophilic CAT-1 even after 8.5 h (Figs. 6 and 7). These results are well in accordance with the notoriously poor skin penetration of compounds with $\log P < 0$ (Schäfer-Korting et al., 2008). Moreover, the penetration rate proves the time dependency of transfer processes which is well in accordance with previous studies using TEMPO and TEMPOL, too (Herrmann et al., 2007).

Loading of the spin probes onto SLN accelerated the transfer considerably for TEMPO (almost complete diffusion into acceptor lipid after 2 h compared to the aqueous solution) and, less pronounced, for TEMPOL (Figs. 5 and 6). The penetration enhancement of lipophilic substances by SLN is already well documented (Küchler et al., 2009b; Lombardi Borgia et al., 2005; Schäfer-Korting et al., 2007). No influence, however, was observed on CAT-1 diffusion in this study (Fig. 7). In contrast, a considerable increase in skin penetration of the hydrophilic dye Rhodamin B was shown when loaded onto SLN (Küchler et al., 2009a). Apparently, the penetration profile of hydrophilic substances differs notably from lipophilic agents. The study showed enhanced penetration most pronounced in the (more polar) viable epidermis (8.8-fold higher values with SLN compared to cream). Considering the stratum corneum the effect was marginal (1.3-fold higher values compared to cream; Küchler et al., 2009a). Obviously the very lipophilic character of the stratum corneum prevents an accumulation of hydrophilic agents like CAT-1 and Rhodamin B but an accumulation in the outermost cell layers of the viable epidermis is possible and facilitated by carrier systems (Küchler et al., 2009a; Moll et al., 2008). Thus, the failure of SLN in this study is explainable by the simplified lipid mixtures used here, just simulating the most superficial and most lipophilic parts of the skin and not the complex system skin.

5. Conclusion

The loading of agents onto SLN is considerably determined by the physicochemical properties and structure of the agents. Lipophilic agents are closely attached to the particle surface, whereas more hydrophilic agents appear to be located within the Poloxamer shell. A dynamic localization of the drug molecules is assumed. The distribution processes at the phase boundaries of carrier and lipids are related to the properties of the applied drug, the lipids and the time.

Acknowledgements

Financial support of the German Research Foundation (FG 463) is gratefully acknowledged. Sarah Küchler was a scholarship holder of the NaFöG program of the city of Berlin.

References

Ahlin, P., Kristl, J., Sentjurc, M., Strancar, J., Pecar, S., 2000. Influence of spin probe structure on its distribution in SLN dispersions. Int. J. Pharm. 196, 241–244.
Blaschke, T., Kankate, L., Kramer, K.D., 2007. Structure and dynamics of drug–carrier systems as studied by parelectric spectroscopy. Adv. Drug Deliv. Rev. 59, 403–410.
Braem, C., Blaschke, T., Panek-Minkin, G., Herrmann, W., Schlupp, P., Paepenmüller, T., Müller-Goyman, C., Mehnert, W., Bittl, R., Schäfer-Korting, M., Kramer, K.D., 2007. Interaction of drug molecules with carrier systems as studied by parelectric spectroscopy and electron spin resonance. J. Control. Release 119, 128–135.
Budil, D.E., Lee, S., Saxena, S., Freed, J., 1996. Nonlinear-least-squares analysis of slow-motion EPR spectra in one or two dimensions using a modified Levenberg–Marquardt algorithm. J. Magn. Res. A 120, 155–189.
Chen, H., Chang, X., Du, D., Liu, W., Liu, J., Weng, T., Yang, Y., Xu, H., Yang, X., 2006. Podophyllotoxin-loaded solid lipid nanoparticles for epidermal targeting. J. Control. Release 110, 296–306.
Degim, T., Hadgraft, J., Ilbasmis, S., Ozkan, Y., 2003. Prediction of skin penetration using artificial neural network (ANN) modeling. J. Pharm. Sci. 92, 656–664.
Herrmann, W., Stosser, R., Borchert, H.H., 2007. ESR imaging investigations of two-phase systems. Magn. Reson. Chem. 45, 496–507.
Jaeckle, E., Schaefer, U.F., Loth, H., 2003. Comparison of effects of different ointment bases on the penetration of ketoprofen through heat-separated human epidermis and artificial lipid barriers. J. Pharm. Sci. 92, 1396–1406.
Jenning, V., Gysler, A., Schäfer-Korting, M., Gohla, S.H., 2000a. Vitamin A loaded solid lipid nanoparticles for topical use: occlusive properties and drug targeting to the upper skin. Eur. J. Pharm. Biopharm. 49, 211–218.
Jenning, V., Schäfer-Korting, M., Gohla, S., 2000b. Vitamin A-loaded solid lipid nanoparticles for topical use: drug release properties. J. Control. Release 66, 115–126.
Jores, K., Mehnert, W., Mader, K., 2003. Physicochemical investigations on solid lipid nanoparticles and on oil-loaded solid lipid nanoparticles: a nuclear magnetic resonance and electron spin resonance study. Pharm. Res. 20, 1274–1283.
Kalariya, M., Padhi, B.K., Chougule, M., Misra, A., 2005. Clobetasol propionate solid lipid nanoparticles cream for effective treatment of eczema: formulation and clinical implications. Indian J. Exp. Biol. 43, 233–240.
Küchler, S., Adbel-Mottaleb, M., Lamprecht, A., Radowski, M.R., Haag, R., Schäfer-Korting, M., 2009a. Influences of nanocarriers' type and size on skin delivery of hydrophilic agents. Int. J. Pharm., doi:10.1016/j.ijpharm.2009.04.046.
Küchler, S., Radowski, M.R., Blaschke, T., Dathe, M., Plendl, J., Haag, R., Schäfer-Korting, M., Kramer, K.D., 2009b. Nanoparticles for skin penetration enhancement—a comparison of a dendritic core–multishell-nanotransporter and solid lipid nanoparticles. Eur. J. Pharm. Biopharm. 71, 243–250.
Kuntsche, J., Bunjes, H., Fahr, A., Pappinen, S., Ronkko, S., Suhonen, M., Urtti, A., 2008. Interaction of lipid nanoparticles with human epidermis and an organotypic cell culture model. Int. J. Pharm. 354, 180–195.
Lamprecht, A., Saulnier, P., Boury, F., Passirani, C., Proust, J.E., Benoit, J.P., 2002. A quantitative method for the determination of amphiphilic drug release kinetics from nanoparticles using a Langmuir balance. Anal. Chem. 74, 3416–3420.
Lombardi Borgia, S., Regehly, M., Sivaramakrishnan, R., Mehnert, W., Korting, H.C., Danker, K., Röder, B., Kramer, K.D., Schäfer-Korting, M., 2005. Lipid nanoparticles for skin penetration enhancement-correlation to drug localization within the particle matrix as determined by fluorescence and parelectric spectroscopy. J. Control. Release 110, 151–163.
Manjunath, K., Reddy, J.S., Venkateswarlu, V., 2005. Solid lipid nanoparticles as drug delivery systems. Methods Find. Exp. Clin. Pharmacol. 27, 127–144.
Moll, K.P., Herrmann, W., Stosser, R., Borchert, H.H., 2008. Changes of the properties in the upper layers of human skin on treatment with models of different pharmaceutical formulations—an ex vivo ESR imaging study. ChemMedChem 3, 653–659.
Müller, R.H., Mäder, K., Gohla, S., 2000. Solid lipid nanoparticles (SLN) for controlled drug delivery—a review of the state of the art. Eur. J. Pharm. Biopharm. 50, 161–177.
Müller, R.H., Radtke, M., Wissing, S.A., 2002. Solid lipid nanoparticles (SLN) and nanostructured lipid carriers (NLC) in cosmetic and dermatological preparations. Adv. Drug Deliv. Rev. 54 (Suppl. 1), S131–155.
Münster, U., Nakamura, C., Haberland, A., Jores, K., Mehnert, W., Rummel, S., Schaller, M., Korting, H.C., Zouboulis Ch, C., Blume-Peytavi, U., Schäfer-Korting, M., 2005. RU 58841-myristate—prodrug development for topical treatment of acne and androgenetic alopecia. Pharmazie 60, 8–12.
Musial, W., Kubis, A., 2003. Preliminary assessment of alginic acid as a factor buffering triethanolamine interacting with artificial skin sebum. Eur. J. Pharm. Biopharm. 55, 237–240.
Potts, R.O., Guy, R.H., 1992. Predicting skin permeability. Pharm. Res. 9, 663–669.
Santos Maia, C., Mehnert, W., Schaller, M., Korting, H.C., Gysler, A., Haberland, A., Schäfer-Korting, M., 2002. Drug targeting by solid lipid nanoparticles for dermal use. J. Drug Target. 10, 489–495.
Schäfer-Korting, M., Bock, U., Diembeck, W., Düsing, H.J., Gamer, A., Haltner-Ukomadu, E., Hoffmann, C., Kaca, M., Kamp, H., Kersen, S., Kietzmann, M., Korting, H.C., Krächter, H.U., Lehr, C.M., Liebsch, M., Mehling, A., Müller-Goymann, C., Netzlaff, F., Niedorf, F., Rübbelke, M.K., Schäfer, U., Schmidt, E., Schreiber, S., Spielmann, H., Vuia, A., Weimer, M., 2008. The use of reconstructed human epidermis for skin absorption testing: results of the validation study. Altern. Lab Anim. 36, 161–187.

Schäfer-Korting, M., Mehnert, W., Korting, H.C., 2007. Lipid nanoparticles for improved topical application of drugs for skin diseases. Adv. Drug Deliv. Rev. 59, 427–443.

Sivaramakrishnan, R., Nakamura, C., Mehnert, W., Korting, H.C., Kramer, K.D., Schäfer-Korting, M., 2004. Glucocorticoid entrapment into lipid carriers—characterisation by parelectric spectroscopy and influence on dermal uptake. J. Control. Release 97, 493–502.

Stecova, J., Mehnert, W., Blaschke, T., Kleuser, B., Sivaramakrishnan, R., Zouboulis, C.C., Seltmann, H., Korting, H.C., Kramer, K.D., Schäfer-Korting, M., 2007. Cyproterone acetate loading to lipid nanoparticles for topical acne treatment: particle characterisation and skin uptake. Pharm. Res. 24, 991–1000.

zur Mühlen, A., Schwarz, C., Mehnert, W., 1998. Solid lipid nanoparticles (SLN) for controlled drug delivery–drug release and release mechanism. Eur. J. Pharm. Biopharm. 45, 149–155.